

Research Article

Performance Analysis of Blind Subspace-Based Signature Estimation Algorithms for DS-CDMA Systems with Unknown Correlated Noise

Keyvan Zarifi and Alex B. Gershman

Department of Communication Systems, Darmstadt University of Technology, Merckstraße 25, 64283 Darmstadt, Germany

Received 3 October 2005; Revised 30 March 2006; Accepted 1 April 2006

Recommended by Vincent Poor

We analyze the performance of two popular blind subspace-based signature waveform estimation techniques proposed by Wang and Poor and Buzzi and Poor for direct-sequence code division multiple-access (DS-CDMA) systems with unknown correlated noise. Using the first-order perturbation theory, analytical expressions for the mean-square error (MSE) of these algorithms are derived. We also obtain simple high SNR approximations of the MSE expressions which explicitly clarify how the performance of these techniques depends on the environmental parameters and how it is related to that of the conventional techniques that are based on the standard white noise assumption. Numerical examples further verify the consistency of the obtained analytical results with simulation results.

Copyright © 2007 K. Zarifi and A. B. Gershman. This is an open access article distributed under the Creative Commons Attribution License, which permits unrestricted use, distribution, and reproduction in any medium, provided the original work is properly cited.

1. INTRODUCTION

In recent years, extensive research efforts have been devoted to develop different strategies for multiuser detection in DS-CDMA systems [1]. One of the most challenging problems in multiuser detection is that of the effect of unknown multipath channel which may result in a significant mismatch between the actual user signature and its presumed value used in the multiuser detection algorithms. Since signature mismatches may cause substantial degradation in the symbol detection performance [2–5], considerable attention has been paid to designing accurate signature estimation techniques at the receiver. These techniques may be classified into the training-based [6, 7] and blind [3, 4, 8–13] methods. In the training-based approaches, each user transmits a sequence of pilot symbols which is known at the receiver where the user signature is estimated by computing the correlation between the received data and this sequence. In nonstationary environments, a reliable signature estimate requires periodic transmission of the pilot sequence. This may cause a considerable reduction of the bandwidth efficiency [2, 3] and has been a strong motivation to develop alternative blind estimation approaches which do not require transmission of the pilot sequence. A promising trend among this type of methods

is the subspace-based techniques [3, 8–11]. The latter techniques exploit the facts that the user signals occupy a low-dimensional subspace in the observation space, and that the signature of each particular user belongs to a subspace defined by its associated spreading code. A typical assumption used in these techniques is that the additive ambient noise is temporally white, and, hence, the signal subspace can be extracted using eigendecomposition of the received data covariance matrix. However, in practice this assumption may be violated [14, 15]. It is well known that in the presence of correlated noise, the signal subspace cannot be identified from the subspace spanned by the eigenvectors associated with the largest eigenvalues of the data covariance matrix. Therefore, some alternative approaches should be employed to identify the signal subspace in the correlated noise case.

One of such approaches has been proposed by Wang and Poor [15]. Their technique is based on the assumption that the receiver contains two well-separated antennas so that the receiver noise is spatially white. Using this fact, the signal subspace can be obtained from the cross-correlation between the received antenna data. Hereafter, we refer to this technique by Wang and Poor as the WP algorithm.

Using a single antenna at the receiver, another technique that addresses the problem of correlated noise has been proposed by Buzzi and Poor [16]. It is based on the assumption that the noise is a circular Gaussian process while the transmitted symbols are noncircular BPSK signals. In such a case, it has been shown in [16] that the signal subspace can be directly identified using the singular value decomposition of the data pseudocovariance matrix. Hereafter, we refer to the technique by Buzzi and Poor as the BP algorithm.

Although the performance of the conventional (white noise assumption-based) signature waveform estimation techniques has been well studied in the literature [9, 10, 17–19], only a little effort has been made to analyze the performance of the estimation algorithms proposed for the unknown correlated noise case. In this paper (see also [20]), we use the first-order perturbation theory to derive approximate expressions for the MSE of the channel vector estimates obtained by the WP and BP algorithms. Under several mild assumptions, simple high SNR approximations of these MSE expressions are also obtained. The derived MSE expressions clarify how the performance of the algorithms depends on the parameters such as the number of data samples, the received power of the user of interest, and the noise covariance matrix. The effect of the spreading factor and the channel length on the performance of the algorithms is also studied. It is shown that the performance of the algorithms depends not only on SNR but also on the direction of the eigenvectors of the noise covariance matrix. To clarify this fact, we fix the eigenvalues of the noise covariance matrix and find the sets of eigenvectors which maximize (minimize) the MSEs of the channel vector estimates. Moreover, over all noise covariance matrices with fixed trace, we obtain those which correspond to the extremal values of the MSEs. It is shown that both the maximum and the minimum values of the MSEs are obtained when the noise covariance matrix is rank deficient. As the trace of the noise covariance matrix is equal to the average noise power, the latter observation shows that the performance of the algorithms may be more sensitive to a low-rank interference than to a full-rank noise with the same average power. We also show that in the presence of white noise, the performances of the WP and BP algorithms are identical to that of the conventional Liu and Xu (LX) algorithm [9] that was developed for the white noise case.

Assuming that the SNR is high and the WP algorithm is used to estimate the channel vector between the user of interest and the first antenna, it is proved that the estimation performance is independent from the noise covariance matrix and the user received power at the second antenna. We use the latter property to show that when the receiver is equipped with multiple antennas, the second antenna can be arbitrarily chosen at high SNRs.

The rest of this paper is organized as follows. In Section 2, we introduce the signal model. A brief overview of the LX, WP, and BP algorithms is provided in Section 3. Section 4 presents our main theoretical results on the performance of the WP and BP algorithms. Simulation results validating our

analysis are presented in Section 5. Conclusions are drawn in Section 6.

2. SIGNAL MODEL

Consider a K -user synchronous DS-CDMA system.¹ The received continuous-time baseband signal can be modelled as [3]

$$x(t) = \sum_{m=-\infty}^{\infty} \sum_{k=1}^K A_k b_k(m) w_k(t - mT_s) + v(t), \quad (1)$$

where T_s is the symbol period, $v(t)$ is the zero-mean additive random noise process, and A_k , $b_k(m)$, and $w_k(t)$ denote the received signal amplitude, the m th data symbol, and the signature waveform of the k th user, respectively. Note that $b_k(m)$ can be drawn from a complex constellation, and hence, in the general case $x(t)$ is complex valued.

Throughout the paper, we use the following common assumptions.

- (A1) The chip sequence period is equal to the symbol period, that is, the short spreading code is considered [22].
- (A2) The user channels are quasistatic, that is, the corresponding impulse channel responses do not change during the whole observation period [9].
- (A3) The duration of the channel impulse response of each user is much shorter than the symbol period T_s , so that the effect of intersymbol-interference (ISI) can be neglected [9, 22].
- (A4) The transmitted symbols and noise are zero-mean random variables. Moreover, transmitted symbols of each user are unit-variance i.i.d. variables, independent from those of the other users, and also independent from the noise [9].

Note that (A1) is common for many multiuser techniques proposed for DS-CDMA systems as most of these algorithms require the received signal $x(t)$ to be cyclostationary. This, in turn, necessitates the use of short spreading codes [23].

Let L_c be the spreading factor and let $\mathbf{c}_k = [c_k[1], c_k[2], \dots, c_k[L_c]]^T$ denote the discrete spreading sequence associated with the k th user where $(\cdot)^T$ stands for the transpose and $c_k[i]$ can be either real or complex valued. According to assumptions (A1) and (A2), the signature waveform of this user can be expressed as [9]

$$w_k(t) = \sum_{l=1}^{L_c} c_k[l] h_k(t - lT_c), \quad (2)$$

where $h_k(t)$ is the channel impulse response of the k th user and $T_c = T_s/L_c$ is the chip period.

¹ The synchronous case is mainly considered for the sake of notational brevity. It is straightforward to extend our analysis to the asynchronous [15] as well as the multiple-antenna [21] DS-CDMA systems.

Let us assume that $h_k(t)$ is zero outside the interval $[0, \alpha T_c]$, where $L - 1 \leq \alpha < L$ and L is a positive integer. From assumption (A3), it follows that $L \ll L_c$. Sampling (1) in the interval corresponding to the n th transmitted symbol of each user and ignoring the first $L - 1$ samples that are contaminated by ISI, the ISI-free received sampled data vector can be written as [9]

$$\mathbf{x}(n) = \sum_{k=1}^K A_k b_k(n) \mathbf{w}_k + \mathbf{v}(n), \quad (3)$$

where $\mathbf{x}(n) = [x(nT_s + LT_c), x(nT_s + (L + 1)T_c), \dots, x(nT_s + L_c T_c)]^T$, $\mathbf{w}_k = [w_k(LT_c), w_k((L + 1)T_c), \dots, w_k(L_c T_c)]^T$, and $\mathbf{v}(n) = [v(nT_s + LT_c), v(nT_s + (L + 1)T_c), \dots, v(nT_s + L_c T_c)]^T$. Note that the similar data model also holds when the effects of chip waveform at the transmitter and chip matched filtering at the receiver are taken into account [21]. Using (2), we have that the signature vector \mathbf{w}_k can be written as

$$\mathbf{w}_k = \begin{bmatrix} c_k[L] & \cdots & c_k[1] \\ c_k[L+1] & \cdots & c_k[2] \\ \vdots & \ddots & \vdots \\ c_k[L_c] & \cdots & c_k[L_c - L + 1] \end{bmatrix} \mathbf{h}_k \triangleq \mathbf{C}_k \mathbf{h}_k, \quad (4)$$

where $\mathbf{h}_k = [h_k(0), h_k(T_c), \dots, h_k((L - 1)T_c)]$. As the spreading code of the user of interest is known at the receiver, if the channel vector \mathbf{h}_k is estimated, then \mathbf{w}_k can be obtained from (4). Hence, throughout this paper we consider the problem of channel vector estimation rather than that of the signature vector estimation. For the sake of consistency, we also assume without any loss of generality that \mathbf{h}_k is a unit Euclidean norm vector ($\|\mathbf{h}_k\| = 1$) [9], that is, the normalization factor is absorbed in A_k . One can present (3) in a more compact form as [9]

$$\mathbf{x}(n) = \mathbf{W}\mathbf{b}(n) + \mathbf{v}(n), \quad (5)$$

where $\mathbf{W} = [A_1 \mathbf{w}_1, A_2 \mathbf{w}_2, \dots, A_K \mathbf{w}_K]$, $\mathbf{b}(n) = [b_1(n), b_2(n), \dots, b_K(n)]^T$.

3. BLIND CHANNEL ESTIMATION

3.1. The LX algorithm

The LX algorithm assumes that the noise is white. In such a case, from assumption (A4) and (5) we have [9]

$$\mathbf{R} \triangleq \mathbb{E}\{\mathbf{x}(n)\mathbf{x}(n)^H\} = \mathbf{W}\mathbf{W}^H + \sigma_v^2 \mathbf{I}, \quad (6)$$

where $\sigma_v^2 \mathbf{I}$ is the noise covariance matrix, \mathbf{I} is the identity matrix, and $\sigma_v^2 = \mathbb{E}\{|v(t)|^2\}$ is the noise variance. The matrix (6) can be eigendecomposed as

$$\mathbf{R} = \begin{bmatrix} \mathbf{U}_s & \mathbf{U}_n \end{bmatrix} \begin{bmatrix} \mathbf{\Omega}_s + \sigma_v^2 \mathbf{I} & \mathbf{0} \\ \mathbf{0} & \sigma_v^2 \mathbf{I} \end{bmatrix} \begin{bmatrix} \mathbf{U}_s^H \\ \mathbf{U}_n^H \end{bmatrix}, \quad (7)$$

where \mathbf{U}_s consists of the eigenvectors associated with the K largest eigenvalues which are the diagonal elements of $\mathbf{\Omega}_s + \sigma_v^2 \mathbf{I}$, and $\mathbf{\Omega}_s$ is a diagonal matrix whose diagonal elements are

the signal subspace eigenvalues. Due to the fact that the noise is white, $\text{range}(\mathbf{W}) = \text{range}(\mathbf{U}_s)$, or, equivalently, \mathbf{U}_s and \mathbf{U}_n span the signal and noise subspaces, respectively.

Without any loss of generality, we assume that \mathbf{h}_1 is the channel vector of interest. As any column of \mathbf{U}_n is orthogonal to all vectors in $\text{range}(\mathbf{U}_s)$, we have [9]

$$\mathbf{U}_n^H \mathbf{w}_1 = \mathbf{T}_1 \mathbf{h}_1 = \mathbf{0}, \quad (8)$$

where $\mathbf{T}_1 \triangleq \mathbf{U}_n^H \mathbf{C}_1$ is an $L_c - L + 1 - K \times L$ matrix. From (8), it follows that \mathbf{T}_1 is not full rank. Assuming that $\text{rank}(\mathbf{T}_1) = L - 1$, the null space of \mathbf{T}_1 is spanned by \mathbf{h}_1 , and, therefore, up to an arbitrary phase rotation, \mathbf{h}_1 can be uniquely determined as a nontrivial solution to (8) subject to $\|\mathbf{h}_1\| = 1$. Note also that if \mathbf{C}_1 is a full-rank matrix, then $\text{rank}(\mathbf{T}_1) = L - 1$ is equivalent to [9]

$$\dim\{\text{range}(\mathbf{C}_1) \cap \text{range}(\mathbf{W})\} = 1, \quad (9)$$

where $\dim\{\cdot\}$ stands for the dimension of a subspace. Equation (9) is the necessary and sufficient condition of signature identifiability using the LX algorithm [9].

In practical scenarios, the data covariance matrix \mathbf{R} is not known exactly and can be estimated as

$$\hat{\mathbf{R}} = \frac{1}{N} \sum_{n=1}^N \mathbf{x}(n)\mathbf{x}(n)^H. \quad (10)$$

As a result, \mathbf{U}_n is estimated as $\hat{\mathbf{U}}_n$ that consists of the eigenvectors associated with the smallest $L_c - L + 1 - K$ eigenvalues of $\hat{\mathbf{R}}$. Substituting $\hat{\mathbf{U}}_n$ in lieu of \mathbf{U}_n in (8) and solving the obtained equation in the least square (LS) sense, we have that the estimated channel vector $\hat{\mathbf{h}}_1$ is given by [9]

$$\hat{\mathbf{h}}_1 = \mathcal{M}\{\mathbf{C}_1^H \hat{\mathbf{U}}_n \hat{\mathbf{U}}_n^H \mathbf{C}_1\}, \quad (11)$$

where $\mathcal{M}\{\cdot\}$ stands for the normalized eigenvector associated with the smallest (minor) eigenvalue. Using the first-order perturbation theory, the mean-square of the encountered estimation error $\delta \mathbf{h}_1 = \hat{\mathbf{h}}_1 - \mathbf{h}_1$ can be approximately written as [18]

$$\mathbb{E}\{\|\delta \mathbf{h}_1\|^2\} \approx \frac{\sigma_v^2}{N} \|\mathbf{T}_1^\dagger\|_F^2 \mathbf{w}_1^H (\mathbf{U}_s \mathbf{\Omega}_s^{-1} \mathbf{U}_s^H + \sigma_v^2 \mathbf{U}_s \mathbf{\Omega}_s^{-2} \mathbf{U}_s^H) \mathbf{w}_1, \quad (12)$$

where \mathbf{T}_1^\dagger is the pseudoinverse of \mathbf{T}_1 and $\|\cdot\|_F$ stands for the Frobenius norm of a matrix. Assuming that the signatures of different users are orthogonal to each other, that is,

$$\mathbf{w}_i^H \mathbf{w}_j = \|\mathbf{w}_i\|^2 \delta_{ij}, \quad (13)$$

where δ_{ij} stands for the Kronecker delta, the MSE expression (12) can be significantly simplified. Note that due to multipath effects, the orthogonality assumption of the signature vectors does not perfectly hold in practice. However, CDMA codes are deliberately designed so that even after passing through a frequency selective channel, the cross correlations between different user signatures are as small as possible.

Hence, in most practical scenarios, (13) is an acceptable assumption [1]. It directly follows from (13) that

$$\mathbf{U}_s = \begin{bmatrix} \frac{\mathbf{w}_1}{\|\mathbf{w}_1\|}, \frac{\mathbf{w}_2}{\|\mathbf{w}_2\|}, \dots, \frac{\mathbf{w}_K}{\|\mathbf{w}_K\|} \end{bmatrix}, \quad (14)$$

$$\mathbf{\Omega}_s = \text{diag}\{A_1^2\|\mathbf{w}_1\|^2, A_2^2\|\mathbf{w}_2\|^2, \dots, A_K^2\|\mathbf{w}_K\|^2\}.$$

Substituting (14) into (12) and using (13) yields

$$\mathbb{E}\{\|\delta\mathbf{h}_1\|^2\} \approx \frac{\sigma_v^2\|\mathbf{T}_1^\dagger\|_F^2}{NA_1^2} \left(1 + \frac{\sigma_v^2}{A_1^2\|\mathbf{w}_1\|^2}\right). \quad (15)$$

If SNR is high enough, that is, $\sigma_v^2 \ll A_1^2\|\mathbf{w}_1\|^2$, the MSE of the channel estimate is further simplified to

$$\mathbb{E}\{\|\delta\mathbf{h}_1\|^2\} \approx \frac{\sigma_v^2\|\mathbf{T}_1^\dagger\|_F^2}{NA_1^2}. \quad (16)$$

Equation (16) can be considered as a reasonable approximation of (12) in the high SNR regime. Note that an expression equivalent to (16) has been derived for the MSE of the estimated signature, $\mathbf{C}_1\hat{\mathbf{h}}_1$, in [9].

3.2. WP algorithm

It is well known that if the white noise assumption does not hold, then the signal subspace is not identical to the subspace spanned by the eigenvectors associated with the K largest eigenvalues of \mathbf{R} and, consequently, the LX algorithm cannot be directly applied to obtain a reliable estimate of \mathbf{h}_1 . To deal with this problem, the WP algorithm assumes that the receiver is equipped with two well-separated antennas such that the noise is *spatially uncorrelated* between them. Similar to (5), the sampled received data vectors are given by

$$\mathbf{x}^{(i)}(n) = \mathbf{W}^{(i)}\mathbf{b}(n) + \mathbf{v}^{(i)}(n), \quad i = 1, 2, \quad (17)$$

where i is the antenna index, $\mathbf{W}^{(i)} = [A_1^{(i)}\mathbf{w}_1^{(i)}, A_2^{(i)}\mathbf{w}_2^{(i)}, \dots, A_K^{(i)}\mathbf{w}_K^{(i)}]$, $\mathbf{v}^{(i)}(n)$ is noise at the i th antenna, and $A_k^{(i)}$ and $\mathbf{w}_k^{(i)} = \mathbf{C}_k\mathbf{h}_k^{(i)}$ are the received amplitude and the signature vector of the k th user at the i th antenna, respectively. The covariance matrix corresponding to the sampled received data vector at each antenna is given by [15]

$$\mathbf{R}^{(i)} \triangleq \mathbb{E}\{\mathbf{x}^{(i)}(n)\mathbf{x}^{(i)H}(n)\} = \mathbf{W}^{(i)}\mathbf{W}^{(i)H} + \mathbf{\Sigma}_v^{(i)}, \quad i = 1, 2, \quad (18)$$

where $\mathbf{\Sigma}_v^{(i)} = \mathbb{E}\{\mathbf{v}^{(i)}(n)\mathbf{v}^{(i)H}(n)\}$. As the noise is uncorrelated between the antennas, we have [15]

$$\begin{aligned} \mathbf{R}^{(12)} &\triangleq \mathbb{E}\{\mathbf{x}^{(1)}(n)\mathbf{x}^{(2)H}(n)\} = \mathbf{W}^{(1)}\mathbf{W}^{(2)H} \\ &= \begin{bmatrix} \mathbf{U}_s^{(1)} & \mathbf{U}_n^{(1)} \end{bmatrix} \begin{bmatrix} \mathbf{\Omega}_s^{(12)} & \mathbf{0} \\ \mathbf{0} & \mathbf{0} \end{bmatrix} \begin{bmatrix} \mathbf{U}_s^{(2)H} \\ \mathbf{U}_n^{(2)H} \end{bmatrix}, \end{aligned} \quad (19)$$

where the right-hand side of (19) is the singular value decomposition (SVD) of $\mathbf{R}^{(12)}$. It is clear that $\text{range}(\mathbf{U}_s^{(1)}) = \text{range}(\mathbf{W}^{(1)})$ and $\text{range}(\mathbf{U}_s^{(2)}) = \text{range}(\mathbf{W}^{(2)})$. For the sake of simplicity but without any loss of generality, let us consider only the channel vector between the first user and the first antenna. Then, we have [15]

$$\mathbf{U}_n^{(1)H}\mathbf{w}_1^{(1)} = \mathbf{T}_1^{(1)}\mathbf{h}_1^{(1)} = \mathbf{0}, \quad (20)$$

where $\mathbf{T}_1^{(1)} \triangleq \mathbf{U}_n^{(1)H}\mathbf{C}_1$ is an $L_c - L + 1 - K \times L$ matrix. If $\text{rank}(\mathbf{T}_1^{(1)}) = L - 1$, then up to an arbitrary phase rotation, $\mathbf{h}_1^{(1)}$ is the unique nontrivial solution to (20) subject to $\|\mathbf{h}_1^{(1)}\| = 1$ [15]. In practice, $\mathbf{R}^{(12)}$ can be estimated as

$$\hat{\mathbf{R}}^{(12)} = \frac{1}{N} \sum_{n=1}^N \mathbf{x}^{(1)}(n)\mathbf{x}^{(2)H}(n) \quad (21)$$

which results in the following estimate of $\mathbf{h}_1^{(1)}$ [15]

$$\hat{\mathbf{h}}_1^{(1)} = \mathcal{M}\{\mathbf{C}_1^H \hat{\mathbf{U}}_n^{(1)} \hat{\mathbf{U}}_n^{(1)H} \mathbf{C}_1\}, \quad (22)$$

where $\hat{\mathbf{U}}_n^{(1)}$ consists of the left singular vectors associated with the $L_c - L + 1 - K$ smallest singular values of $\hat{\mathbf{R}}^{(12)}$.

3.3. BP algorithm

Another approach to solve the problem of channel estimation in presence of unknown correlated noise has been proposed in [16]. Without requiring the second antenna, this algorithm is based on the assumption that the transmitted symbols are drawn from the BPSK constellation ($b_k(n) = \pm 1$) and the noise is a circular Gaussian process. It directly follows from the latter assumption that

$$\mathbb{E}\{\mathbf{v}(n)\mathbf{v}(n)^T\} = \mathbf{0}. \quad (23)$$

Let $\tilde{\mathbf{R}} \triangleq \mathbb{E}\{\mathbf{x}(n)\mathbf{x}^T(n)\}$ be the pseudocovariance matrix of the sampled received data. Using (5) along with (23), we have [16]

$$\tilde{\mathbf{R}} = \mathbf{W}\mathbf{W}^T = \begin{bmatrix} \tilde{\mathbf{U}}_s & \tilde{\mathbf{U}}_n \end{bmatrix} \begin{bmatrix} \tilde{\mathbf{\Omega}}_s & \mathbf{0} \\ \mathbf{0} & \mathbf{0} \end{bmatrix} \begin{bmatrix} \tilde{\mathbf{V}}_s^H \\ \tilde{\mathbf{V}}_n^H \end{bmatrix}, \quad (24)$$

where $\tilde{\mathbf{\Omega}}_s$ is a diagonal matrix whose diagonal elements are the nonzero singular values of $\tilde{\mathbf{R}}$ and the columns of $\tilde{\mathbf{U}}_s$ are the corresponding left singular vectors. It is easy to show that $\text{range}(\tilde{\mathbf{U}}_s) = \text{range}(\mathbf{W})$ [16], and, hence,

$$\tilde{\mathbf{U}}_n^H \mathbf{w}_1 = \tilde{\mathbf{T}}_1 \mathbf{h}_1 = \mathbf{0}, \quad (25)$$

where $\tilde{\mathbf{T}}_1 \triangleq \tilde{\mathbf{U}}_n^H \mathbf{C}_1$. It can be observed that $\tilde{\mathbf{T}}_1$ is an $L_c - L + 1 - K \times L$ matrix and the unique identification of \mathbf{h}_1 from (25) requires that $\text{rank}(\tilde{\mathbf{T}}_1) = L - 1$ [16]. In practice, similar to the LX and WP algorithms, \mathbf{h}_1 can be estimated by

$$\hat{\mathbf{h}}_1 = \mathcal{M}\{\mathbf{C}_1^H \hat{\tilde{\mathbf{U}}}_n \hat{\tilde{\mathbf{U}}}_n^H \mathbf{C}_1\}, \quad (26)$$

where $\widehat{\mathbf{U}}_n$ is the matrix containing the left singular vectors associated with the $L_c - L + 1 - K$ least singular values of $\widehat{\mathbf{R}}$, and

$$\widehat{\mathbf{R}} = \frac{1}{N} \sum_{n=1}^N \mathbf{x}(n)\mathbf{x}(n)^T \quad (27)$$

is the sample estimate of $\widetilde{\mathbf{R}}$.

4. PERFORMANCE ANALYSIS

4.1. WP algorithm

In order to evaluate the performance of the WP algorithm, we use the first-order perturbation theory to prove the following theorem.

Theorem 1. *Assume that $\mathbf{h}_1^{(1)}$ is estimated using (22). Then, the first-order perturbation theory-based approximation of the MSE of the estimation error $\delta\mathbf{h}_1^{(1)} = \widehat{\mathbf{h}}_1^{(1)} - \mathbf{h}_1^{(1)}$ is given by*

$$E \left\{ \|\delta\mathbf{h}_1^{(1)}\|^2 \right\} \approx \frac{1}{N} \text{tr}(\boldsymbol{\Sigma}_v^{(1)}\boldsymbol{\Psi}) \mathbf{w}_1^{(1)H} \mathbf{R}^{(12)\dagger H} \mathbf{R}^{(2)} \mathbf{R}^{(12)\dagger} \mathbf{w}_1^{(1)}, \quad (28)$$

where $\text{tr}(\cdot)$ stands for the trace of a matrix and

$$\boldsymbol{\Psi} \triangleq \mathbf{U}_n^{(1)} \mathbf{T}_1^{(1)\dagger H} \mathbf{T}_1^{(1)\dagger} \mathbf{U}_n^{(1)H}. \quad (29)$$

Moreover, if the following conditions hold:

$$\mathbf{w}_k^{(i)H} \mathbf{w}_l^{(i)} = \|\mathbf{w}_k^{(i)}\|^2 \delta_{kl}, \quad i = 1, 2, \quad (30)$$

$$\lambda_{\max}(\boldsymbol{\Sigma}_v^{(2)}) \ll (A_1^{(2)} \|\mathbf{w}_1^{(2)}\|)^2, \quad (31)$$

then (28) reduces to

$$E \left\{ \|\delta\mathbf{h}_1^{(1)}\|^2 \right\} \approx \frac{\text{tr}(\boldsymbol{\Sigma}_v^{(1)}\boldsymbol{\Psi})}{NA_1^{(1)2}}, \quad (32)$$

where $\lambda_{\max}(\cdot)$ stands for the maximum eigenvalue.

Proof. See Appendix A. \square

Note that the average received power of the first user at the second antenna is equal to the right-hand side of (31), while the average noise power at the same antenna is lower bounded by the left-hand side because

$$E \left\{ \|\mathbf{v}^{(2)}(n)\|^2 \right\} = \text{tr}(\boldsymbol{\Sigma}_v^{(2)}) \geq \lambda_{\max}(\boldsymbol{\Sigma}_v^{(2)}). \quad (33)$$

Hence, if SNR at the second antenna is reasonably high, it is guaranteed that (31) holds. Using this observation along with the fact that (30) approximately holds in most practical scenarios, we can view (32) as a simple approximation of (28) in the high SNR regime. It explicitly clarifies the MSE of the estimated channel vector in terms of the *environmental parameters* such as the received power of the user of interest at the first antenna, the number of data samples as well as the noise covariance matrix $\boldsymbol{\Sigma}_v^{(1)}$.

Note that both the MSE expressions (28) and (32) depend on $\boldsymbol{\Sigma}_v^{(1)}$ only through $\text{tr}(\boldsymbol{\Sigma}_v^{(1)}\boldsymbol{\Psi})$. To study the parameters which have impact on the value of $\text{tr}(\boldsymbol{\Sigma}_v^{(1)}\boldsymbol{\Psi})$, we first should note that if the channel vector is uniquely identifiable, then $\text{rank}(\mathbf{T}_1^{(1)}) = \text{rank}(\boldsymbol{\Psi}) = L - 1$. Moreover, we have

$$\tau \triangleq \dim\{\text{null}(\boldsymbol{\Psi})\} = L_c - L + 1 - \text{rank}(\boldsymbol{\Psi}) = L_c - 2(L - 1), \quad (34)$$

where $\text{null}(\cdot)$ stands for the null-space of a matrix.² The effects of different parameters on the value of $\text{tr}(\boldsymbol{\Sigma}_v^{(1)}\boldsymbol{\Psi})$ are separately clarified in the following discussion.

Effects of L_c and L

As $\boldsymbol{\Sigma}_v^{(1)}$ and $\boldsymbol{\Psi}$ are positive (semi-) definite matrices, it follows that $\text{tr}(\boldsymbol{\Sigma}_v^{(1)}\boldsymbol{\Psi})$ is real and nonnegative. Note that the projection of $\boldsymbol{\Sigma}_v^{(1)}$ onto $\text{null}(\boldsymbol{\Psi})$ does not have any effect on the value of $\text{tr}(\boldsymbol{\Sigma}_v^{(1)}\boldsymbol{\Psi})$ which depends only on the projection of $\boldsymbol{\Sigma}_v^{(1)}$ onto $\text{range}(\boldsymbol{\Psi})$. Therefore, the larger the projection of $\boldsymbol{\Sigma}_v^{(1)}$ onto $\text{null}(\boldsymbol{\Psi})$, the smaller the value of $\text{tr}(\boldsymbol{\Sigma}_v^{(1)}\boldsymbol{\Psi})$. Using the latter fact, the effect of the spreading factor and the channel length on $\text{tr}(\boldsymbol{\Sigma}_v^{(1)}\boldsymbol{\Psi})$, and, consequently, on the performance of the WP algorithm can be explained as follows. From (34) it can be observed that if either the spreading factor L_c increases or the channel length L decreases, then $\dim\{\text{null}(\boldsymbol{\Psi})\}$ increases. In the latter case, the projection of the columns of $\boldsymbol{\Sigma}_v^{(1)}$ onto $\text{null}(\boldsymbol{\Psi})$ becomes larger, and, therefore, their contribution to the value of $\text{tr}(\boldsymbol{\Sigma}_v^{(1)}\boldsymbol{\Psi})$ becomes smaller.

Effect of the eigenvectors of $\boldsymbol{\Sigma}_v^{(1)}$

The directions of the eigenvectors of $\boldsymbol{\Sigma}_v^{(1)}$ with respect to the eigenvectors of $\boldsymbol{\Psi}$ have a considerable impact on the value of $\text{tr}(\boldsymbol{\Sigma}_v^{(1)}\boldsymbol{\Psi})$. To show this, let us eigendecompose $\boldsymbol{\Psi}$ as

$$\boldsymbol{\Psi} = \boldsymbol{\Pi}\boldsymbol{\Theta}\boldsymbol{\Pi}^H, \quad (35)$$

where $\boldsymbol{\Pi} = [\boldsymbol{\pi}_1 \ \boldsymbol{\pi}_2 \ \cdots \ \boldsymbol{\pi}_{L-1}]$ is an $L_c - L + 1 \times L - 1$ matrix whose columns are the orthonormal eigenvectors associated with the decreasingly-ordered positive eigenvalues of $\boldsymbol{\Psi}$ that are the diagonal elements of $\boldsymbol{\Theta} = \text{diag}\{\theta_1, \theta_2, \dots, \theta_{L-1}\}$. In contrary to $\text{rank}(\boldsymbol{\Psi})$, $m \triangleq \text{rank}(\boldsymbol{\Sigma}_v^{(1)})$ may not be known. In fact, $\text{rank}(\boldsymbol{\Sigma}_v^{(1)})$ may vary from $m = 1$ for the case of coherent interference to $m = L_c - L + 1$ for the case of full-rank noise. Let us consider an arbitrary value of m and eigendecompose $\boldsymbol{\Sigma}_v^{(1)}$ as

$$\boldsymbol{\Sigma}_v^{(1)} = \mathbf{U}_v \boldsymbol{\Gamma}_v \mathbf{U}_v^H, \quad (36)$$

where \mathbf{U}_v is an $L_c - L + 1 \times m$ matrix whose orthonormal columns are the eigenvectors associated with the decreasingly-ordered positive eigenvalues of $\boldsymbol{\Sigma}_v^{(1)}$ which are the diagonal elements of $\boldsymbol{\Gamma}_v = \text{diag}\{\gamma_1, \gamma_2, \dots, \gamma_m\}$.

² It should be noticed from (29) that $\text{range}(\mathbf{W}^{(1)})$ is a K -dimensional subspace in $\text{null}(\boldsymbol{\Psi})$.

The value of $\text{tr}(\Sigma_v^{(1)}\Psi)$, and, hence, the MSE expressions (28) and (32) critically depend on the direction of the columns of \mathbf{U}_v relative to the columns of $\mathbf{\Pi}$. To explain this fact, let us fix the matrix Γ_v and find the matrices $\mathbf{U}_{v\max}$ and $\mathbf{U}_{v\min}$ which maximize and minimize $\text{tr}(\Sigma_v^{(1)}\Psi)$, respectively. It can be shown [24, 25] that

$$\max_{\mathbf{U}_v} \{\text{tr}(\Sigma_v^{(1)}\Psi)\} = \sum_{i=1}^{\tau_1} \gamma_i \theta_i, \quad \tau_1 = \min\{L-1, m\}, \quad (37)$$

and $\mathbf{U}_{v\max}$ is given by

$$\mathbf{U}_{v\max} = \begin{cases} [\boldsymbol{\pi}_1 \ \boldsymbol{\pi}_2 \ \cdots \ \boldsymbol{\pi}_m], & \text{if } m \leq L-1, \\ \begin{bmatrix} \mathbf{\Pi} & \mathbf{\Pi}_{m-L+1}^\perp \end{bmatrix}, & \text{if } m > L-1, \end{cases} \quad (38)$$

where $\mathbf{\Pi}_l^\perp$ is an $L_c - L + 1 \times l$ matrix whose $l \leq \tau$ columns are *arbitrarily* chosen from a set of τ orthonormal vectors in $\text{null}(\Psi)$. According to (38), for a fixed Γ_v , the MSE expressions (28) and (32) are maximal if the first τ_1 columns of \mathbf{U}_v and $\mathbf{\Pi}$ coincide. In turn, we have [24, 25]

$$\min_{\mathbf{U}_v} \{\text{tr}(\Sigma_v^{(1)}\Psi)\} = \begin{cases} 0, & \text{if } m \leq \tau, \\ \sum_{i=1}^{m-\tau} \gamma_{\tau+i} \theta_{L-i}, & \text{if } m > \tau, \end{cases} \quad (39)$$

and $\mathbf{U}_{v\min}$ is given by

$$\mathbf{U}_{v\min} = \begin{cases} \mathbf{\Pi}_m^\perp, & \text{if } m \leq \tau, \\ \begin{bmatrix} \mathbf{\Pi}_\tau^\perp & \boldsymbol{\pi}_{L-1} & \cdots & \boldsymbol{\pi}_{L-(m-\tau)} \end{bmatrix}, & \text{if } m > \tau. \end{cases} \quad (40)$$

According to (40), the necessary condition to minimize the MSE expressions (28) and (32) is that the first $\tau_2 \triangleq \min\{m, \tau\}$ columns of \mathbf{U}_v are in $\text{null}(\Psi)$. Note that the matrix $\Sigma_{v\min} = \mathbf{U}_{v\min} \Gamma_v \mathbf{U}_{v\min}^H$ has the maximum projection onto $\text{null}(\Psi)$, that is, the space spanned by the eigenvectors associated with the τ_2 largest eigenvalues of $\Sigma_{v\min}$ is in $\text{null}(\Psi)$.

Assuming that the average noise power at the first antenna is given by e_o , that is,

$$\mathbb{E} \{ \|\mathbf{v}^{(1)}(n)\|^2 \} = \text{tr}(\Sigma_v^{(1)}) = \sum_{i=1}^m \gamma_i = e_o, \quad (41)$$

we can also obtain the extremal values of the MSE expressions (28) and (32) as follows. Since for any pair of positive (semi-) definite matrices $\Sigma_v^{(1)}$ and Ψ we have [25]

$$\text{tr}(\Sigma_v^{(1)}\Psi) \leq \lambda_{\max}(\Psi) \text{tr}(\Sigma_v^{(1)}), \quad (42)$$

it directly follows that

$$\text{tr}(\Sigma_v^{(1)}\Psi) \leq \theta_1 e_o, \quad (43)$$

where, assuming that the largest eigenvalue of Ψ is unique, (43) holds with equality if and only if

$$\Sigma_v^{(1)} = e_o \boldsymbol{\pi}_1 \boldsymbol{\pi}_1^H. \quad (44)$$

Moreover, it is obvious that among all noise covariance matrices with $\sum_{i=1}^m \gamma_i = e_o$, those in the form of

$$\Sigma_v^{(1)} = \mathbf{\Pi}_m^\perp \Gamma_v \mathbf{\Pi}_m^H \quad (45)$$

result in the MSE expressions (28) and (32) equal to zero. It is interesting to observe from (44) and (45) that, given the average noise power at the first antenna, both the maximal and the minimal values of the MSE of the channel vector estimate are obtained when the noise covariance matrix is rank deficient. As a rank deficient covariance matrix can be attributed to a narrow-band interference, it follows that the performance of the WP algorithm can be more sensitive to a narrow-band interference than a full-rank colored noise.

Now, let us consider two important particular scenarios in which the WP algorithm may be used and discuss the pertaining results.

White noise scenario: if the noise at the first antenna is white, that is, $\Sigma_v^{(1)} = \sigma_v^{(1)2} \mathbf{I}$, then (32) reduces to

$$\mathbb{E} \{ \|\delta \mathbf{h}_1^{(1)}\|^2 \} \approx \frac{\sigma_v^{(1)2} \|\mathbf{T}^{(1)\dagger}\|_F^2}{NA_1^{(1)2}} \quad (46)$$

which is equal to the derived MSE of the LX algorithm in (16). Hence, even though the WP algorithm is proposed to estimate the channel vector in the presence of unknown correlated noise, it is also applicable to the white noise scenario. In the latter case, the performance of the WP algorithm is identical to that of the LX algorithm.

Multiple antenna systems: it follows from (32) that if the SNR at the second antenna is high enough so that (31) holds, then the MSE of the channel vector estimate between the user of interest and the first antenna is independent of $\Sigma_v^{(2)}$ and the received power of this user at the second antenna. Let us consider a receiver with $M > 2$ antennas which are spatially separated so that the noises between the first antenna and all the other antennas are uncorrelated. Moreover, assume that the SNR is high enough:

$$\lambda_{\max}(\Sigma_v^{(i)}) \ll (A_1^{(i)} \|\mathbf{w}_1^{(i)}\|)^2, \quad i = 2, \dots, M, \quad (47)$$

and that we aim to estimate the channel vector between the first user and the first antenna using the WP algorithm. Since this algorithm is based on processing of the data cross-correlation matrix between the first antenna and another well-separated *auxiliary* antenna, we have to choose the auxiliary antenna among the $M-1$ available antennas. However, it directly follows from (32) that if the aforementioned assumptions hold, the performance of the channel vector estimate is insensitive to the choice of such an antenna, that is, the auxiliary antenna can be chosen *arbitrarily*.

4.2. BP algorithm

The following theorem quantizes the performance of the BP algorithm.

Theorem 2. *Assume that the channel vector is estimated using the BP algorithm. Then, the first-order perturbation theory-based approximation of the MSE of the estimation error*

$\delta \mathbf{h}_1 = \hat{\mathbf{h}}_1 - \mathbf{h}_1$ is given by

$$\mathbb{E} \{ \|\delta \mathbf{h}_1\|^2 \} \approx \frac{1}{N} \mathbf{w}_1^H \tilde{\mathbf{R}}^{\dagger H} \{ \text{tr}(\mathbf{\Sigma}_v \tilde{\Psi}) \mathbf{R}^T + (\mathbf{\Sigma}_v \tilde{\Psi} \mathbf{\Sigma}_v)^T \} \tilde{\mathbf{R}}^{\dagger} \mathbf{w}_1, \quad (48)$$

where

$$\mathbf{\Sigma}_v = \mathbb{E} \{ \mathbf{v}(n) \mathbf{v}(n)^H \}, \quad (49)$$

$$\mathbf{R} = \mathbf{W} \mathbf{W}^H + \mathbf{\Sigma}_v, \quad (50)$$

$$\tilde{\Psi} \triangleq \tilde{\mathbf{U}}_n \tilde{\mathbf{T}}_1^{\dagger H} \tilde{\mathbf{T}}_1^{\dagger} \tilde{\mathbf{U}}_n^H. \quad (51)$$

Moreover, if (13) holds and

$$\lambda_{\max}(\mathbf{\Sigma}_v) \ll A_1^2 \|\mathbf{w}_1\|^2, \quad (52)$$

then (48) reduces to

$$\mathbb{E} \{ \|\delta \mathbf{h}_1\|^2 \} \approx \frac{\text{tr}(\mathbf{\Sigma}_v \tilde{\Psi})}{N A_1^2}. \quad (53)$$

Proof. See Appendix B. \square

As can be observed from (53), in the high SNR regime the MSE of the channel vector estimate of the BP algorithm can be expressed in terms of the noise covariance matrix, power of the received signal, and the number of data samples.

Note that if the channel vector is uniquely identifiable from the BP algorithm, we have $\text{rank}(\tilde{\Psi}) = L-1$. Comparing (53) with (32), it can be readily shown that the effect of the spreading factor and the channel length on both the WP and BP algorithms are similar. Moreover, following a discussion similar to that of Section 4.1, we can obtain the extremal values of $\text{tr}(\mathbf{\Sigma}_v \tilde{\Psi})$, and, consequently, those of the MSE expression (53). Let us first eigendecompose $\tilde{\Psi}$ as

$$\tilde{\Psi} = \tilde{\mathbf{\Pi}} \tilde{\mathbf{\Theta}} \tilde{\mathbf{\Pi}}^H, \quad (54)$$

where $\tilde{\mathbf{\Pi}} = [\tilde{\boldsymbol{\pi}}_1 \ \tilde{\boldsymbol{\pi}}_2 \ \cdots \ \tilde{\boldsymbol{\pi}}_{L-1}]$ contains the orthonormal eigenvectors associated with the positive eigenvalues of $\tilde{\Psi}$ and $\tilde{\mathbf{\Theta}} = \text{diag}\{\tilde{\theta}_1, \tilde{\theta}_2, \dots, \tilde{\theta}_{L-1}\}$ is the diagonal matrix that contains the decreasingly-ordered positive eigenvalues. Let us denote $q \triangleq \text{rank}(\mathbf{\Sigma}_v)$ and eigendecompose $\mathbf{\Sigma}_v$ as

$$\mathbf{\Sigma}_v = \tilde{\mathbf{U}}_v \tilde{\mathbf{\Gamma}}_v \tilde{\mathbf{U}}_v^H, \quad (55)$$

where $\tilde{\mathbf{U}}_v$ contains the orthonormal eigenvectors associated with the positive eigenvalues of $\mathbf{\Sigma}_v$ which are ordered decreasingly as the diagonal elements of $\tilde{\mathbf{\Gamma}}_v = \text{diag}\{\tilde{\gamma}_1, \tilde{\gamma}_2, \dots, \tilde{\gamma}_q\}$. Denoting $\tilde{\mathbf{\Pi}}_1^{\perp}$ as an $L_c - L + 1 \times l$ matrix whose columns are orthonormal vectors in $\text{null}(\tilde{\Psi})$, we have

(i) for any given $\tilde{\mathbf{\Gamma}}_v$,

$$\max_{\tilde{\mathbf{U}}_v} \{ \text{tr}(\mathbf{\Sigma}_v \tilde{\Psi}) \} = \sum_{i=1}^{\tilde{\tau}_1} \tilde{\gamma}_i \tilde{\theta}_i, \quad \tilde{\tau}_1 = \min\{L-1, q\}, \quad (56)$$

where the matrix $\tilde{\mathbf{U}}_v$ which maximizes $\text{tr}(\mathbf{\Sigma}_v \tilde{\Psi})$ is

$$\tilde{\mathbf{U}}_{v, \max} = \begin{cases} [\tilde{\boldsymbol{\pi}}_1 \ \tilde{\boldsymbol{\pi}}_2 \ \cdots \ \tilde{\boldsymbol{\pi}}_q], & \text{if } q \leq L-1, \\ [\tilde{\mathbf{\Pi}} \ \tilde{\mathbf{\Pi}}_{q-L+1}^{\perp}], & \text{if } q > L-1; \end{cases} \quad (57)$$

(ii) for any given $\tilde{\mathbf{\Gamma}}_v$,

$$\min_{\tilde{\mathbf{U}}_v} \{ \text{tr}(\mathbf{\Sigma}_v \tilde{\Psi}) \} = \begin{cases} 0, & \text{if } q \leq \tau, \\ \sum_{i=1}^{q-\tau} \tilde{\gamma}_{\tau+i} \tilde{\theta}_{L-i}, & \text{if } q > \tau, \end{cases} \quad (58)$$

where the matrix $\tilde{\mathbf{U}}_v$ which minimizes $\text{tr}(\mathbf{\Sigma}_v \tilde{\Psi})$ is

$$\tilde{\mathbf{U}}_{v, \min} = \begin{cases} \tilde{\mathbf{\Pi}}_q^{\perp}, & \text{if } q \leq \tau, \\ [\tilde{\mathbf{\Pi}}_{\tau}^{\perp} \ \tilde{\boldsymbol{\pi}}_{L-1} \ \cdots \ \tilde{\boldsymbol{\pi}}_{L-(q-\tau)}], & \text{if } q > \tau. \end{cases} \quad (59)$$

Comparing (56)–(59) with (37)–(40), it can be observed that the conclusions which follow (37)–(40) can be easily extended to the BP algorithm, and, hence, we do not repeat them for the sake of brevity.

Let us also consider the case that the average noise power is given by e_o , that is, $\text{tr}(\mathbf{\Sigma}_v) = \sum_{i=1}^q \tilde{\gamma}_i = e_o$. In such a case, assuming that the largest eigenvalue of $\tilde{\Psi}$ is unique, the noise covariance matrix which maximizes $\text{tr}(\mathbf{\Sigma}_v \tilde{\Psi})$ is given by

$$\mathbf{\Sigma}_v = e_o \tilde{\boldsymbol{\pi}}_1 \tilde{\boldsymbol{\pi}}_1^H. \quad (60)$$

Moreover, over all noise covariance matrices $\mathbf{\Sigma}_v$ with $\sum_{i=1}^q \tilde{\gamma}_i = e_o$, the value of $\text{tr}(\mathbf{\Sigma}_v \tilde{\Psi})$ and, consequently, that of the MSE expression (53) is zero if and only if

$$\mathbf{\Sigma}_v = \tilde{\mathbf{\Pi}}_q^{\perp} \tilde{\mathbf{\Gamma}}_v \tilde{\mathbf{\Pi}}_q^{\perp H}. \quad (61)$$

Similar to the WP algorithm, it follows from (60) and (61) that the performance of the BP algorithm can be more sensitive to the narrow-band interference than to the full-rank noise.

If noise is white, that is, $\mathbf{\Sigma}_v = \sigma_v^2 \mathbf{I}$, the MSE expression (53) reduces to

$$\mathbb{E} \{ \|\delta \mathbf{h}_1\|^2 \} \approx \frac{\sigma_v^2 \|\tilde{\mathbf{T}}_1^{\dagger}\|_F^2}{N A_1^2}. \quad (62)$$

Hence, the performances of the BP and the LX algorithms are identical in the white noise scenario. Therefore, the BP algorithm can also be applied to estimate the channel vector in the white noise case without any estimation performance loss as compared to the conventional LX algorithm.

Another interesting relationship between the WP and BP algorithms follows from comparing (32) and (53). Let the users transmit BPSK modulated symbols and let the receiver be equipped with two well-separated antennas such that noise is spatially uncorrelated between them. Also, let

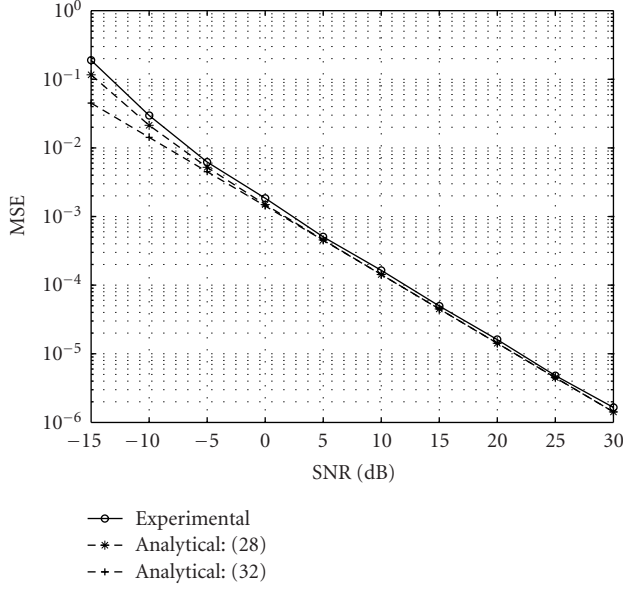


FIGURE 1: The MSE of the estimated channel versus SNR. The WP algorithm.

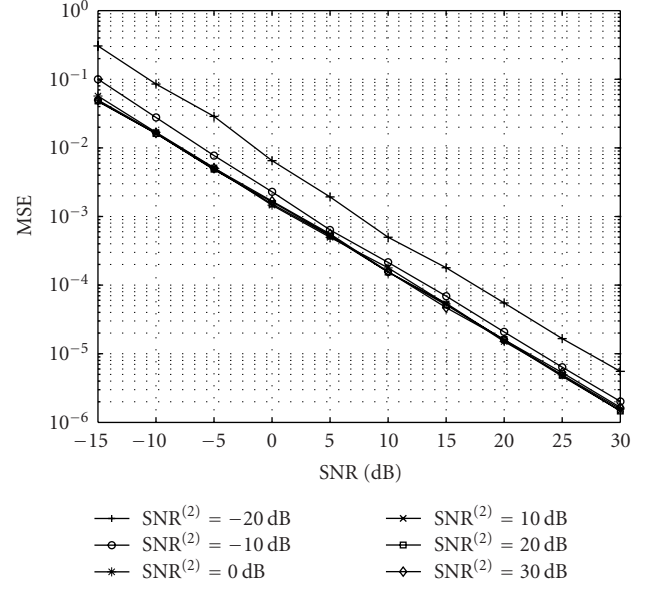


FIGURE 3: The MSE of the estimated channel versus SNR at the first antenna for different values of SNR at the second antenna. The WP algorithm.

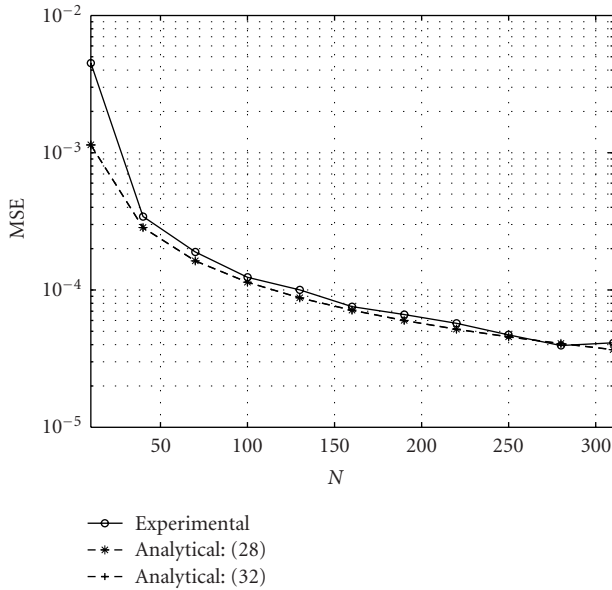


FIGURE 2: The MSE of the estimated channel versus number of data samples. The WP algorithm.

(30) and (31) hold and

$$\lambda_{\max}(\Sigma_v^{(1)}) \ll (A_1^{(1)} \|\mathbf{w}_1^{(1)}\|)^2. \quad (63)$$

Then, the MSE expressions (32) and (53) can be readily verified to coincide in the following two cases: when $\mathbf{h}_1^{(1)}$ is estimated using the WP algorithm with both antennas, and when $\mathbf{h}_1^{(1)}$ is estimated using the BP algorithm with only the first antenna.

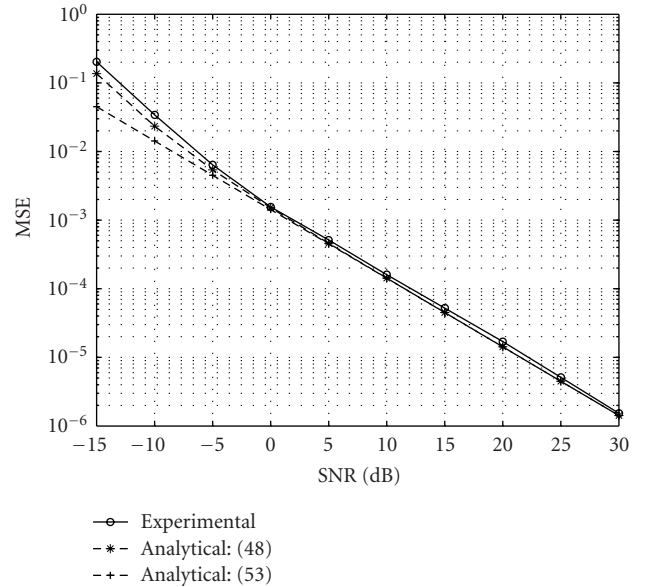


FIGURE 4: The MSE of the estimated channel versus SNR. The BP algorithm.

5. SIMULATIONS

In this section, we validate our analytical results via computer simulations. In all the examples, we consider $K = 7$ synchronous CDMA users that transmit BPSK-modulated symbols. Each point of the simulation curves is the result of averaging over 200 Monte-Carlo realizations of the noise and transmission data sequences. In Figures 1–8, Gold codes of length $L_c = 31$ are employed as the user spreading sequences

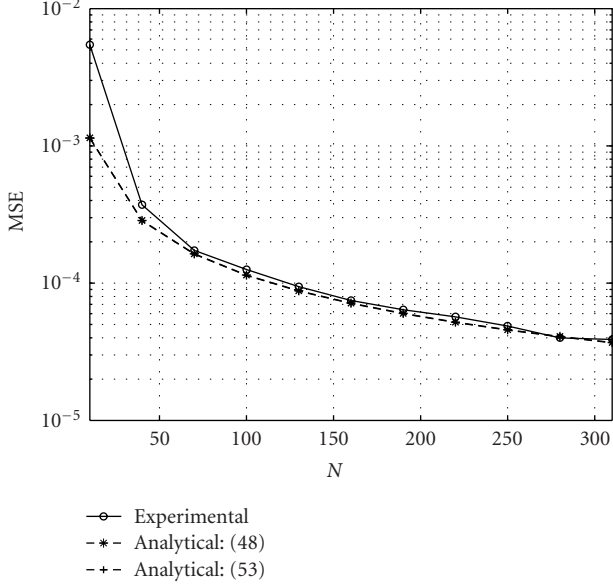


FIGURE 5: The MSE of the estimated channel versus number of data samples. The BP algorithm.

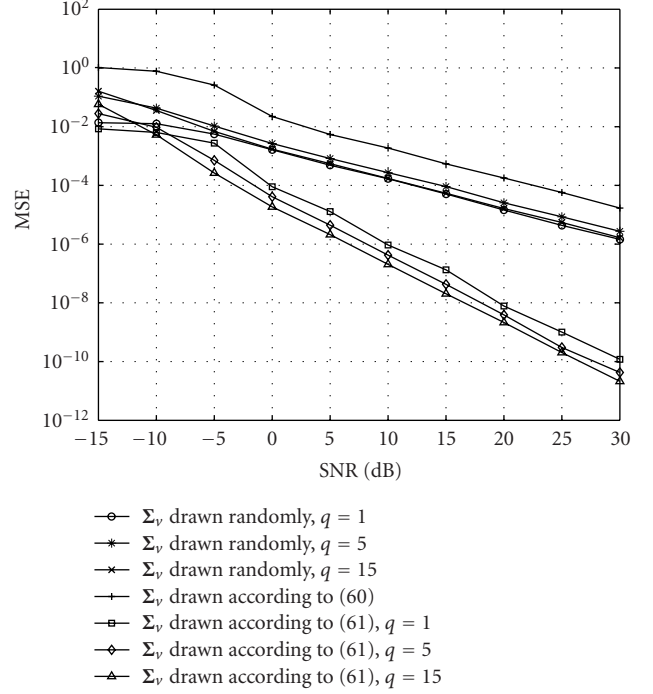


FIGURE 7: MSEs of the estimated channel versus SNR for $e_o = 28$ and different matrices Σ_v . The BP algorithm.

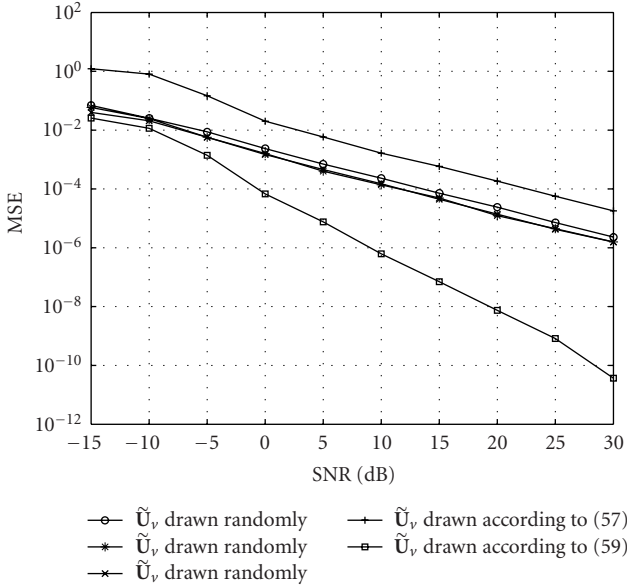


FIGURE 6: The MSE of the estimated channel versus SNR for $\tilde{\Gamma}_v = \text{diag}\{20, 5, 3\}$ and different matrices $\tilde{\mathbf{U}}_v$. The BP algorithm.

and channel vectors of length $L = 4$ are independently drawn from a zero-mean white complex Gaussian process and then are scaled to become unit-norm vectors. The ambiguity in the phase of the channel vector estimate is resolved by assuming that the phase of the first tap of the channel vector is known at the receiver. In Figures 1–5 and 9, the received noise at each antenna is considered to be a circular Gaussian process such that $[\Sigma_v]_{ij}$, the (i, j) th entry of its covariance matrix, is equal to $0.7^{|i-j|}$. In the figures where the MSE of

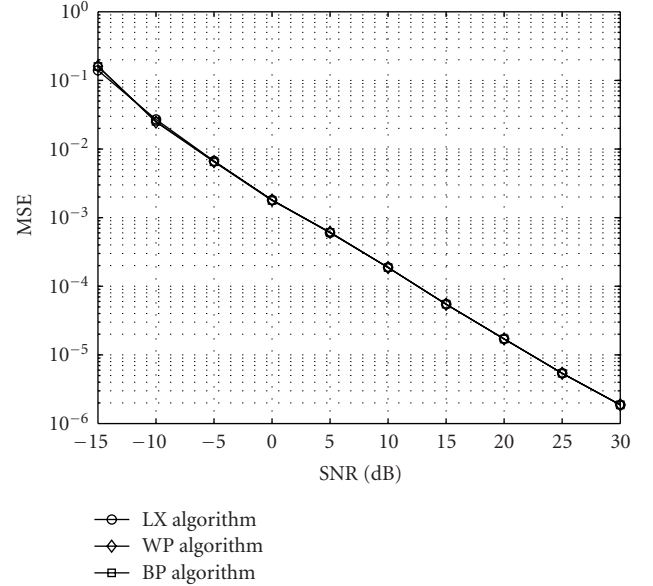


FIGURE 8: MSEs of the estimated channel versus SNR in the white noise environment. The LX, WP, and BP algorithms.

the channel estimate is drawn versus SNR, it is assumed that $N = 80$ data samples are used to estimate the channel.

Figures 1–3 illustrate the accuracy of our analytical results derived for the WP algorithm. In Figure 1, it is assumed that SNRs of all users at both antennas are identical and $\mathbf{h}_1^{(1)}$ is estimated according to (22). The solid curve represents the

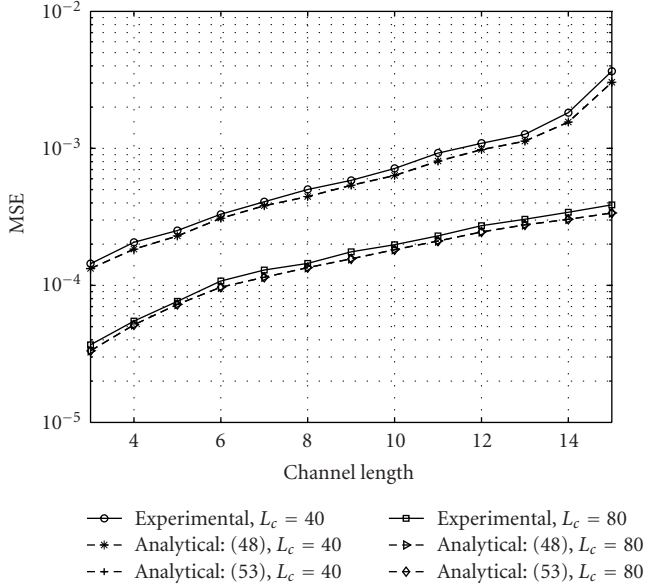


FIGURE 9: MSEs of the estimated channel versus L for $L_c = 40$ and $L_c = 80$. The BP algorithm.

MSE resulting from this estimate. This curve is compared with our analytical results given by (28) and (32). It can be observed that both theoretical curves follow the experimental MSE curve with a good precision. Note that when the SNR is very low, the channel vector estimation error is quite large and, hence, it could not be reliably predicted using the first-order perturbation theory. In such a condition, the analytical MSE curves obtained from (28) and (32) show a considerable discrepancy with the experimental MSE curve.

Figure 2 depicts the experimental and the analytical MSE curves versus the number of data samples N . In this figure, it is assumed that the received signal power from each user at each of the two antennas is equal to 10 dB. Due to the fact that SNR is reasonably high, the theoretical curve (28) and its high SNR approximation (32) are almost indistinguishable from each other and they follow the experimental MSE curve with a good accuracy. It can be observed from Figure 2 that, when the number of data samples N is small, the small perturbation assumption is violated, and, hence, the accuracy of the analytical MSE curves decreases.

Figure 3 shows the MSE of the estimated channel $\hat{\mathbf{h}}_1^{(1)}$ versus SNR at the first antenna ($\text{SNR}^{(1)}$) for 6 different values of SNR at the second antenna ($\text{SNR}^{(2)}$). As expected from Section 4.1, the performance of the channel estimation is almost independent from the exact value of $\text{SNR}^{(2)}$, unless $\text{SNR}^{(2)}$ is very low.

Figures 4–7 and 9 show the performance of the BP algorithm and compare it to our analytical results. In Figure 4, the experimental MSE curve is plotted versus SNR and is compared with the theoretical curves obtained from (48) and (53). As can be observed from the figure, the two theoretical MSE curves are very close to each other and also closely

follow the experimental MSE curve for the SNRs higher than 0 dB.

Figure 5 shows the experimental and the theoretical curves drawn versus the number of data samples N for SNR equal to 10 dB. As the figure shows, the theoretical curve (48) is precisely followed by its high SNR approximation (53) and both of them are very close to the experimental MSE curve.

Figure 6 shows the experimental MSE curves versus SNR for noise covariance matrices with identical $\tilde{\mathbf{\Gamma}}_v = \text{diag}\{20, 5, 3\}$ and different matrices of eigenvectors $\tilde{\mathbf{U}}_v$. Three random realizations of $\tilde{\mathbf{U}}_v$ as well as $\tilde{\mathbf{U}}_{v_{\max}}$ and $\tilde{\mathbf{U}}_{v_{\min}}$ are drawn and then using (55) the corresponding noise covariance matrices are obtained. The BP algorithm is used to estimate the channel vector in the presence of a correlated noise with the so-obtained noise covariance matrices. Figure 6 confirms our theoretical results in Section 4.2 which state that the worst and the best MSE performances are obtained when $\tilde{\mathbf{U}}_v = \tilde{\mathbf{U}}_{v_{\max}}$ and $\tilde{\mathbf{U}}_v = \tilde{\mathbf{U}}_{v_{\min}}$, respectively. Note that if $\tilde{\mathbf{U}}_v = \tilde{\mathbf{U}}_{v_{\min}}$, then, unlike the MSE expression (53), the experimental MSE performance is not equal to zero. It is due to the fact that the MSE expression (53) is obtained using the first-order perturbation theory and even in the high SNR regime this expression has a slight difference with the experimental MSE.

Figure 7 plots the experimental MSE curves versus SNR for noises with identical average energy of $e_o = L_c - L + 1 = 28$ and different covariance matrices. For each value of $q = 1, 5$, and 15, one noise covariance matrix is drawn randomly and another one is obtained according to (61). A rank-one noise covariance matrix is also derived according to (60). Then, the BP algorithm is used to estimate the channel vector in the presence of correlated noise with the so-obtained noise covariance matrices. Our analytical results in Section 4.2 are validated by observing that the worst and the best MSE performances are obtained when the noise covariance matrix follows (60) and (61), respectively.

In Figure 8, the performances of the LX, WP, and BP algorithms are tested in the white noise environment. As predicted by our analysis in Section 4, all three methods have a nearly identical performance.

Figure 9 shows the experimental and the theoretical MSE curves of the BP algorithm versus the channel length L for two different values of the spreading factors $L_c = 40$ and $L_c = 80$. In this example, we use random spreading codes rather than the optimized Gold codes. The entries of these codes are randomly drawn from the set $\{-1, +1\}$. From Figure 9 we see that, as predicted in Section 4, the estimation performance decreases with increasing L . When $L_c = 80$, the MSE of the channel vector estimate is significantly lower than that for $L_c = 40$. It can be observed that the curves corresponding to (48) and (53) are quite close to each other and, therefore, the use of the random spreading codes instead of the Gold codes retains the accuracy of (53).

6. CONCLUSIONS

In this paper, analytical expressions for the MSE of the signature waveform estimation techniques of [15, 16] have been

derived. Assuming that different user signature vectors are orthogonal, the simplified versions of these expressions have been also obtained for the high SNR regime. The effect of the correlated noise on the performance of both algorithms has been studied. It has been shown that the direction of the eigenvectors of the noise covariance matrix has a significant effect on the performance of both algorithms. In particular, assuming that the eigenvalues of the noise covariance matrix are fixed, the noise covariance matrix eigenvectors corresponding to the extremal values of the MSEs have been obtained. Over all noise covariance matrices with identical average noise power, the extremal values of the MSEs have been derived and it has been shown that both the maximal and the minimal values of the MSEs are achieved when the noise covariance matrix is rank deficient. Moreover, it has been shown that at high SNRs and in the presence of white noise, the performance of these two techniques is identical to that of the conventional white noise-based technique of [9].

In the high SNR regime, it has been proved that the performance of the technique proposed in [15] is independent from the noise covariance matrix and the user received power at the second auxiliary antenna. This property has been generalized to the multiple antenna systems and it has been shown that for such systems the choice of the auxiliary antenna is arbitrary at high SNRs.

APPENDICES

A. PROOF OF THEOREM 1

Since $\mathbf{U}_n^{(1)}$ spans the null-space of $\mathbf{R}^{(12)}$, we have

$$\mathbf{U}_n^{(1)H} \mathbf{W}^{(1)} = \mathbf{0}. \quad (\text{A.1})$$

Equations (A.1) and (29) yield

$$\Psi \mathbf{W}^{(1)} = \mathbf{W}^{(1)H} \Psi = \mathbf{0}. \quad (\text{A.2})$$

To prove (28), we introduce

$$\delta \mathbf{R}^{(12)} \triangleq \hat{\mathbf{R}}^{(12)} - \mathbf{R}^{(12)}, \quad (\text{A.3})$$

$$\delta \mathbf{U}_n^{(1)} \triangleq \hat{\mathbf{U}}_n^{(1)} - \mathbf{U}_n^{(1)}. \quad (\text{A.4})$$

Using the perturbation theory, the first-order approximation of $\delta \mathbf{U}_n^{(1)}$ can be written as [9, 26, 27]

$$\delta \mathbf{U}_n^{(1)} \approx -\mathbf{R}^{(12)\dagger H} \delta \mathbf{R}^{(12)H} \mathbf{U}_n^{(1)}, \quad (\text{A.5})$$

where

$$\mathbf{R}^{(12)\dagger} = \mathbf{U}_s^{(2)} \mathbf{\Omega}_s^{(12)-1} \mathbf{U}_s^{(1)H}. \quad (\text{A.6})$$

Since

$$\hat{\mathbf{U}}_n^{(1)H} \mathbf{C}_1 \hat{\mathbf{h}}_1^{(1)} \approx \mathbf{0}, \quad (\text{A.7})$$

it follows that the first-order estimate of $\delta \mathbf{h}_1^{(1)}$ is given by

$$\delta \mathbf{h}_1^{(1)} \approx -\mathbf{T}_1^{(1)\dagger} \delta \mathbf{U}_n^{(1)H} \mathbf{w}_1^{(1)}. \quad (\text{A.8})$$

Inserting (A.5) into (A.8) and applying the expectation operation to the squared norm of the resulting expression, we have

$$\begin{aligned} & \mathbb{E} \{ \|\delta \mathbf{h}_1^{(1)}\|^2 \} \\ & \approx \mathbf{w}_1^{(1)H} \mathbf{R}^{(12)\dagger H} \mathbb{E} \{ \delta \mathbf{R}^{(12)H} \Psi \delta \mathbf{R}^{(12)} \} \mathbf{R}^{(12)\dagger} \mathbf{w}_1^{(1)}. \end{aligned} \quad (\text{A.9})$$

Let us introduce

$$\Xi \triangleq \mathbb{E} \{ \delta \mathbf{R}^{(12)H} \Psi \delta \mathbf{R}^{(12)} \}. \quad (\text{A.10})$$

From (A.2) and (A.3) it follows that

$$\Xi = \mathbb{E} \{ \hat{\mathbf{R}}^{(12)H} \Psi \hat{\mathbf{R}}^{(12)} \}. \quad (\text{A.11})$$

Using (17) and (21) in (A.11) yields

$$\begin{aligned} \Xi &= \frac{1}{N^2} \sum_{j=1}^N \sum_{k=1}^N \mathbb{E} \{ (\mathbf{W}^{(2)} \mathbf{b}(j) + \mathbf{v}^{(2)}(j)) \\ & \quad \times (\mathbf{b}(j)^H \mathbf{W}^{(1)H} + \mathbf{v}^{(1)H}(j)) \Psi \\ & \quad \times (\mathbf{W}^{(1)} \mathbf{b}(k) + \mathbf{v}^{(1)}(k)) \\ & \quad \times (\mathbf{b}(k)^H \mathbf{W}^{(2)H} + \mathbf{v}^{(2)H}(k)) \}. \end{aligned} \quad (\text{A.12})$$

Using (A.2) to simplify the resulting expression, we obtain

$$\Xi = \frac{1}{N} (\Phi_1 + \Phi_2), \quad (\text{A.13})$$

where

$$\begin{aligned} \Phi_1 &\triangleq \mathbb{E} \{ \mathbf{W}^{(2)} \mathbf{b}(j) \mathbf{v}^{(1)H}(j) \Psi \mathbf{v}^{(1)}(j) \mathbf{b}^H(j) \mathbf{W}^{(2)H} \}, \\ \Phi_2 &\triangleq \mathbb{E} \{ \mathbf{v}^{(2)}(j) \mathbf{v}^{(1)H}(j) \Psi \mathbf{v}^{(1)}(j) \mathbf{v}^{(2)H}(j) \}. \end{aligned} \quad (\text{A.14})$$

We also have

$$\begin{aligned} \Phi_1 &= \mathbb{E} \{ \mathbf{v}^{(1)H}(j) \Psi \mathbf{v}^{(1)}(j) \} \mathbf{W}^{(2)} \mathbf{W}^{(2)H} \\ &= \mathbb{E} \{ \text{tr} \left(\mathbf{v}^{(1)H}(j) \Psi \mathbf{v}^{(1)}(j) \right) \} \mathbf{W}^{(2)} \mathbf{W}^{(2)H} \\ &= \text{tr} \left(\mathbb{E} \{ \mathbf{v}^{(1)}(j) \mathbf{v}^{(1)H}(j) \Psi \} \right) \mathbf{W}^{(2)} \mathbf{W}^{(2)H} \\ &= \text{tr} (\mathbf{\Sigma}_v^{(1)} \Psi) \mathbf{W}^{(2)} \mathbf{W}^{(2)H}, \\ \Phi_2 &= \mathbb{E} \{ \mathbf{v}^{(1)H}(j) \Psi \mathbf{v}^{(1)}(j) \} \mathbb{E} \{ \mathbf{v}^{(2)}(j) \mathbf{v}^{(2)H}(j) \} \\ &= \text{tr} (\mathbf{\Sigma}_v^{(1)} \Psi) \mathbf{\Sigma}_v^{(2)}. \end{aligned} \quad (\text{A.15})$$

Substituting (A.15) into (A.13) and using (18), we obtain

$$\Xi = \frac{1}{N} \text{tr} (\mathbf{\Sigma}_v^{(1)} \Psi) \mathbf{R}^{(2)}. \quad (\text{A.16})$$

Using (A.16) in (A.9) directly yields (28). To prove (32), first we use (19) and (30) to obtain

$$\begin{aligned} \mathbf{U}_s^{(1)} &= \left[\frac{\mathbf{w}_1^{(1)}}{\|\mathbf{w}_1^{(1)}\|}, \dots, \frac{\mathbf{w}_K^{(1)}}{\|\mathbf{w}_K^{(1)}\|} \right], \\ \mathbf{\Omega}_s^{(12)} &= \text{diag} \{ A_1^{(1)} A_1^{(2)} \|\mathbf{w}_1^{(1)}\| \|\mathbf{w}_1^{(2)}\|, \dots, A_K^{(1)} A_K^{(2)} \|\mathbf{w}_K^{(1)}\| \|\mathbf{w}_K^{(2)}\| \}, \\ \mathbf{U}_s^{(2)} &= \left[\frac{\mathbf{w}_1^{(2)}}{\|\mathbf{w}_1^{(2)}\|}, \dots, \frac{\mathbf{w}_K^{(2)}}{\|\mathbf{w}_K^{(2)}\|} \right]. \end{aligned} \quad (\text{A.17})$$

Let

$$\check{\mathbf{w}}_1^{(1)} \triangleq \mathbf{R}^{(12)\dagger} \mathbf{w}_1^{(1)} = \mathbf{U}_s^{(2)} \mathbf{\Omega}_s^{(12)-1} \mathbf{U}_s^{(1)H} \mathbf{w}_1^{(1)}. \quad (\text{A.18})$$

Substituting (A.17) into (A.18) and using (30), we have

$$\check{\mathbf{w}}_1^{(1)} = \frac{1}{A_1^{(1)} A_1^{(2)} \|\mathbf{w}_1^{(2)}\|^2} \mathbf{w}_1^{(2)}. \quad (\text{A.19})$$

Using (A.19) along with (28) yields

$$\mathbb{E} \left\{ \|\delta \mathbf{h}_1^{(1)}\|^2 \right\} \approx \frac{\text{tr}(\mathbf{\Sigma}_v^{(1)} \mathbf{\Psi})}{N A_1^{(1)2} A_1^{(2)2} \|\mathbf{w}_1^{(2)}\|^4} \mathbf{w}_1^{(2)H} \mathbf{R}^{(2)} \mathbf{w}_1^{(2)}. \quad (\text{A.20})$$

Substituting $\mathbf{R}^{(2)}$ from (18) into (A.20) and using (30) to simplify the result, we obtain

$$\mathbb{E} \left\{ \|\delta \mathbf{h}_1^{(1)}\|^2 \right\} \approx \frac{\text{tr}(\mathbf{\Sigma}_v^{(1)} \mathbf{\Psi})}{N A_1^{(1)2}} \left(1 + \frac{\mathbf{w}_1^{(2)H} \mathbf{\Sigma}_v^{(2)} \mathbf{w}_1^{(2)}}{A_1^{(2)2} \|\mathbf{w}_1^{(2)}\|^4} \right). \quad (\text{A.21})$$

As for any $\mathbf{w}_1^{(2)}$ and $\mathbf{\Sigma}_v^{(2)}$,

$$\mathbf{w}_1^{(2)H} \mathbf{\Sigma}_v^{(2)} \mathbf{w}_1^{(2)} \leq \|\mathbf{w}_1^{(2)}\|^2 \lambda_{\max}(\mathbf{\Sigma}_v^{(2)}), \quad (\text{A.22})$$

then, when (31) holds, (32) directly follows from (A.21). This completes the proof.

B. PROOF OF THEOREM 2

According to (24), we have

$$\tilde{\mathbf{U}}_n^H \mathbf{W} = \mathbf{0}. \quad (\text{B.1})$$

From (51) along with (B.1) it follows that

$$\tilde{\mathbf{\Psi}} \mathbf{W} = \mathbf{W}^H \tilde{\mathbf{\Psi}} = \mathbf{0}. \quad (\text{B.2})$$

Using the procedure similar to that in Appendix A, it can be readily shown that

$$\mathbb{E} \left\{ \|\delta \mathbf{h}_1\|^2 \right\} \approx \mathbf{w}_1^H \tilde{\mathbf{R}}^\dagger \mathbf{E} \left\{ \delta \tilde{\mathbf{R}}^H \tilde{\mathbf{\Psi}} \delta \tilde{\mathbf{R}} \right\} \tilde{\mathbf{R}}^\dagger \mathbf{w}_1, \quad (\text{B.3})$$

where

$$\delta \tilde{\mathbf{R}} \triangleq \hat{\tilde{\mathbf{R}}} - \tilde{\mathbf{R}}. \quad (\text{B.4})$$

Let us denote

$$\tilde{\tilde{\mathbf{E}}} \triangleq \mathbb{E} \left\{ \delta \tilde{\mathbf{R}}^H \tilde{\mathbf{\Psi}} \delta \tilde{\mathbf{R}} \right\}. \quad (\text{B.5})$$

Substituting (B.4) into (B.5), and then using (B.2) to simplify the result, we have

$$\tilde{\tilde{\mathbf{E}}} = \mathbb{E} \left\{ \hat{\tilde{\mathbf{R}}}^H \tilde{\mathbf{\Psi}} \hat{\tilde{\mathbf{R}}} \right\}. \quad (\text{B.6})$$

Expanding the right-hand side of (B.6) according to (27), and then using (B.2) to simplify the resulting expression, we obtain

$$\tilde{\tilde{\mathbf{E}}} = \frac{1}{N} (\tilde{\Phi}_1 + \tilde{\Phi}_2), \quad (\text{B.7})$$

where

$$\tilde{\Phi}_1 \triangleq \mathbb{E} \left\{ \mathbf{v}^H(i) \tilde{\mathbf{\Psi}} \mathbf{v}(i) \mathbf{W}^* \mathbf{b}(i) \mathbf{b}^T(i) \mathbf{W}^T \right\}, \quad (\text{B.8})$$

$$\tilde{\Phi}_2 \triangleq \mathbb{E} \left\{ \mathbf{v}^*(i) \mathbf{v}^H(i) \tilde{\mathbf{\Psi}} \mathbf{v}(i) \mathbf{v}^T(i) \right\}, \quad (\text{B.9})$$

and $(\cdot)^*$ stands for the conjugate. Since the transmitted symbols are drawn from the BPSK constellation, we have

$$\begin{aligned} \tilde{\Phi}_1 &= \mathbb{E} \left\{ \mathbf{v}^H(i) \tilde{\mathbf{\Psi}} \mathbf{v}(i) \right\} \mathbf{W}^* \mathbf{W}^T, \\ &= \text{tr}(\mathbf{\Sigma}_v \tilde{\mathbf{\Psi}}) \mathbf{W}^* \mathbf{W}^T, \end{aligned} \quad (\text{B.10})$$

where the second line of (B.10) can be derived using the same steps as in (A.15). To obtain $\tilde{\Phi}_2$, it can be easily shown from (B.9) that

$$[\tilde{\Phi}_2]_{kl} = \sum_{g=1}^{L_c-L+1} \sum_{m=1}^{L_c-L+1} [\tilde{\mathbf{\Psi}}]_{gm} \mathbb{E} \left\{ [\mathbf{v}]_k^* [\mathbf{v}]_g^* [\mathbf{v}]_m [\mathbf{v}]_l \right\}, \quad (\text{B.11})$$

where $[\cdot]_k$ is the k th entry of a vector and the time index i has been dropped from $\mathbf{v}(i)$ for the sake of simplicity. Since \mathbf{v} is a multivariate circular Gaussian random vector, we have [28]

$$\begin{aligned} \mathbb{E} \left\{ [\mathbf{v}]_k^* [\mathbf{v}]_g^* [\mathbf{v}]_m [\mathbf{v}]_l \right\} &= \mathbb{E} \left\{ [\mathbf{v}]_m [\mathbf{v}^*]_k \right\} \mathbb{E} \left\{ [\mathbf{v}]_l [\mathbf{v}^*]_g \right\} \\ &\quad + \mathbb{E} \left\{ [\mathbf{v}]_m [\mathbf{v}^*]_g \right\} \mathbb{E} \left\{ [\mathbf{v}]_l [\mathbf{v}^*]_k \right\} \\ &= [\mathbf{\Sigma}_v]_{mk} [\mathbf{\Sigma}_v]_{lg} + [\mathbf{\Sigma}_v]_{mg} [\mathbf{\Sigma}_v]_{lk}. \end{aligned} \quad (\text{B.12})$$

Substituting (B.12) into (B.11), we obtain

$$\begin{aligned} [\tilde{\Phi}_2]_{kl} &= \sum_{g=1}^{L_c-L+1} [\mathbf{\Sigma}_v]_{lg} [\tilde{\mathbf{\Psi}} \mathbf{\Sigma}_v]_{gk} + [\tilde{\mathbf{\Psi}} \mathbf{\Sigma}_v]_{gg} [\mathbf{\Sigma}_v]_{lk} \\ &= [\mathbf{\Sigma}_v \tilde{\mathbf{\Psi}} \mathbf{\Sigma}_v]_{lk} + \text{tr}(\tilde{\mathbf{\Psi}} \mathbf{\Sigma}_v) [\mathbf{\Sigma}_v]_{lk}. \end{aligned} \quad (\text{B.13})$$

From (B.13) it directly follows that

$$\tilde{\Phi}_2 = (\mathbf{\Sigma}_v \tilde{\mathbf{\Psi}} \mathbf{\Sigma}_v)^T + \text{tr}(\tilde{\mathbf{\Psi}} \mathbf{\Sigma}_v) \mathbf{\Sigma}_v^T. \quad (\text{B.14})$$

Substituting (B.10) and (B.14) into (B.7) and using the resulting expression in (B.3), we obtain (48).

To prove (53), we note that (13) along with (24) yield

$$\begin{aligned} \tilde{\mathbf{U}}_s &= \left[\frac{\mathbf{w}_1}{\|\mathbf{w}_1\|}, \dots, \frac{\mathbf{w}_K}{\|\mathbf{w}_K\|} \right], \\ \tilde{\mathbf{\Omega}}_s &= \text{diag} \left\{ A_1^2 \|\mathbf{w}_1\|^2, \dots, A_K^2 \|\mathbf{w}_K\|^2 \right\}, \\ \tilde{\mathbf{V}}_s &= \left[\frac{\mathbf{w}_1^*}{\|\mathbf{w}_1\|}, \dots, \frac{\mathbf{w}_K^*}{\|\mathbf{w}_K\|} \right]. \end{aligned} \quad (\text{B.15})$$

Let us denote

$$\check{\mathbf{w}}_1 \triangleq \tilde{\mathbf{R}}^\dagger \mathbf{w}_1 = \tilde{\mathbf{V}}_s \tilde{\mathbf{\Omega}}_s^{-1} \tilde{\mathbf{U}}_s^H \mathbf{w}_1. \quad (\text{B.16})$$

Substituting (B.15) into the right-hand side of (B.16) and using (13), we have

$$\check{\mathbf{w}}_1 = \frac{\mathbf{w}_1^*}{A_1^2 \|\mathbf{w}_1\|^2}. \quad (\text{B.17})$$

Using (B.17) in (48) results in the following expression for $E\{\|\delta\mathbf{h}_1\|^2\}$:

$$E\{\|\delta\mathbf{h}_1\|^2\} \approx \frac{\text{tr}(\tilde{\Psi}\Sigma_v)}{N\|\mathbf{w}_1\|^2 A_1^4} (\alpha_1 + \alpha_2 + \alpha_3), \quad (\text{B.18})$$

where

$$\begin{aligned} \alpha_1 &\triangleq \frac{\mathbf{w}_1^T}{\|\mathbf{w}_1\|} \mathbf{W}^* \mathbf{W}^T \frac{\mathbf{w}_1^*}{\|\mathbf{w}_1\|}, \\ \alpha_2 &\triangleq \frac{\mathbf{w}_1^T}{\|\mathbf{w}_1\|} \Sigma_v^T \frac{\mathbf{w}_1^*}{\|\mathbf{w}_1\|}, \\ \alpha_3 &\triangleq \frac{1}{\text{tr}(\tilde{\Psi}\Sigma_v)} \frac{\mathbf{w}_1^T}{\|\mathbf{w}_1\|} (\Sigma_v \tilde{\Psi} \Sigma_v)^T \frac{\mathbf{w}_1^*}{\|\mathbf{w}_1\|}. \end{aligned} \quad (\text{B.19})$$

It directly follows from (13) that

$$\alpha_1 = A_1^2 \|\mathbf{w}_1\|^2. \quad (\text{B.20})$$

Noting that both Σ_v and $\tilde{\Psi}$ are positive (semi-) definite matrices, it is easy to find an upper-bound for α_2 and α_3 as

$$\begin{aligned} \alpha_2 &= \left(\frac{\mathbf{w}_1^H}{\|\mathbf{w}_1\|} \Sigma_v \frac{\mathbf{w}_1}{\|\mathbf{w}_1\|} \right)^* \leq \lambda_{\max}^*(\Sigma_v) = \lambda_{\max}(\Sigma_v), \\ \alpha_3 &= \frac{1}{\text{tr}(\tilde{\Psi}\Sigma_v)} \left(\frac{\mathbf{w}_1^H}{\|\mathbf{w}_1\|} (\Sigma_v \tilde{\Psi} \Sigma_v) \frac{\mathbf{w}_1}{\|\mathbf{w}_1\|} \right)^* \\ &\leq \frac{1}{\text{tr}(\tilde{\Psi}\Sigma_v)} \lambda_{\max}^*(\Sigma_v \tilde{\Psi} \Sigma_v) \\ &= \frac{1}{\text{tr}(\tilde{\Psi}\Sigma_v)} \lambda_{\max}(\Sigma_v \tilde{\Psi} \Sigma_v) \\ &\leq \frac{\lambda_{\max}(\tilde{\Psi}\Sigma_v)}{\text{tr}(\tilde{\Psi}\Sigma_v)} \lambda_{\max}(\Sigma_v) \leq \lambda_{\max}(\Sigma_v). \end{aligned} \quad (\text{B.21})$$

Hence, if (52) holds, both α_2 and α_3 are negligible comparing to α_1 . Substituting (B.20) into (B.18) directly yields (53). This completes the proof.

ACKNOWLEDGMENTS

This work was supported by the Wolfgang Paul Award Program of the Alexander von Humboldt Foundation and German Ministry of Education and Research.

REFERENCES

- [1] S. Verdú, *Multuser Detection*, Cambridge University Press, Cambridge, UK, 1998.
- [2] M. Honig, U. Madhow, and S. Verdú, "Blind adaptive multiuser detection," *IEEE Transactions on Information Theory*, vol. 41, no. 4, pp. 944–960, 1995.
- [3] X. Wang and H. V. Poor, "Blind multiuser detection: a subspace approach," *IEEE Transactions on Information Theory*, vol. 44, no. 2, pp. 677–690, 1998.
- [4] Z. Xu, P. Liu, and X. Wang, "Blind multiuser detection: from MOE to subspace methods," *IEEE Transactions on Signal Processing*, vol. 52, no. 2, pp. 510–524, 2004.
- [5] K. Zarifi, S. Shahbazpanahi, A. B. Gershman, and Z.-Q. Luo, "Robust blind multiuser detection based on the worst-case performance optimization of the MMSE receiver," *IEEE Transactions on Signal Processing*, vol. 53, no. 1, pp. 295–305, 2005.
- [6] U. Madhow and M. L. Honig, "MMSE interference suppression for direct-sequence spread-spectrum CDMA," *IEEE Transactions on Communications*, vol. 42, no. 12, pp. 3178–3188, 1994.
- [7] U. Mitra and H. V. Poor, "Adaptive receiver algorithms for near-far resistant CDMA," *IEEE Transactions on Communications*, vol. 43, no. 2–4, part 3, pp. 1713–1724, 1995.
- [8] S. E. Bensley and B. Aazhang, "Subspace-based channel estimation for code division multiple access communication systems," *IEEE Transactions on Communications*, vol. 44, no. 8, pp. 1009–1020, 1996.
- [9] H. Liu and G. Xu, "Subspace method for signature waveform estimation in synchronous CDMA systems," *IEEE Transactions on Communications*, vol. 44, no. 10, pp. 1346–1354, 1996.
- [10] M. Torlak and G. Xu, "Blind multiuser channel estimation in asynchronous CDMA systems," *IEEE Transactions on Signal Processing*, vol. 45, no. 1, pp. 137–147, 1997.
- [11] X. Wang and H. V. Poor, "Blind equalization and multiuser detection in dispersive CDMA channels," *IEEE Transactions on Communications*, vol. 46, no. 1, pp. 91–103, 1998.
- [12] Z. Xu and M. K. Tsatsanis, "Blind adaptive algorithms for minimum variance CDMA receivers," *IEEE Transactions on Communications*, vol. 49, no. 1, pp. 180–194, 2001.
- [13] Q. Li, C. N. Georghiadis, and X. Wang, "Blind multiuser detection in uplink CDMA with multipath fading: a sequential EM approach," *IEEE Transactions on Communications*, vol. 52, no. 1, pp. 71–81, 2004.
- [14] S. Buzzi, M. Lops, and H. V. Poor, "Code-aided interference suppression for DS/CDMA overlay systems," *Proceedings of the IEEE*, vol. 90, no. 3, pp. 394–435, 2002.
- [15] X. Wang and H. V. Poor, "Blind joint equalization and multiuser detection for DS-CDMA in unknown correlated noise," *IEEE Transactions on Circuits and Systems for Video Technology II*, vol. 46, no. 7, pp. 886–895, 1999.
- [16] S. Buzzi and H. V. Poor, "A single-antenna blind receiver for multiuser detection in unknown correlated noise," *IEEE Transactions on Vehicular Technology*, vol. 51, no. 1, pp. 209–215, 2002.
- [17] N. Yuen and B. Friedlander, "Asymptotic performance analysis for signature waveform estimation in synchronous CDMA systems," *IEEE Transactions on Signal Processing*, vol. 46, no. 6, pp. 1753–1757, 1998.
- [18] Z. Xu, "On the second-order statistics of the weighted sample covariance matrix," *IEEE Transactions on Signal Processing*, vol. 51, no. 2, pp. 527–534, 2003.
- [19] Z. Xu, "Effects of imperfect blind channel estimation on performance of linear CDMA receivers," *IEEE Transactions on Signal Processing*, vol. 52, no. 10, part 1, pp. 2873–2884, 2004.
- [20] K. Zarifi and A. B. Gershman, "Performance analysis of subspace-based signature waveform estimation algorithms for DS-CDMA systems with unknown correlated noise," in *Proceedings of 6th IEEE Workshop on Signal Processing Advances in Wireless Communications (SPAWC '05)*, pp. 600–604, New York, NY, USA, June 2005.
- [21] A. Host-Madsen, X. Wang, and S. Bahng, "Asymptotic analysis of blind multiuser detection with blind channel estimation," *IEEE Transactions on Signal Processing*, vol. 52, no. 6, pp. 1722–1738, 2004.

- [22] M. Honig and M. K. Tsatsanis, "Adaptive techniques for multiuser CDMA receivers," *IEEE Signal Processing Magazine*, vol. 17, no. 3, pp. 49–61, 2000.
- [23] S. Parkvall, "Variability of user performance in cellular DS-SS-CDMA-long versus short spreading sequences," *IEEE Transactions on Communications*, vol. 48, no. 7, pp. 1178–1187, 2000.
- [24] I. D. Coope and P. F. Renaud, "Trace inequalities with applications to orthogonal regression and matrix nearness problems," Report UCDMS2000/17, Department of Mathematics and Statistics, University of Canterbury, Christchurch, New Zealand, November 2000, <http://www.math.canterbury.ac.nz/research/ucdms2000n17.pdf>.
- [25] R. A. Horn and C. R. Johnson, *Matrix Analysis*, Cambridge University Press, Cambridge, UK, 1999.
- [26] F. Li, H. Liu, and R. J. Vaccaro, "Performance analysis for DOA estimation algorithms: unification, simplification, and observations," *IEEE Transactions on Aerospace and Electronic Systems*, vol. 29, no. 4, pp. 1170–1184, 1993.
- [27] Z. Xu, "Perturbation analysis for subspace decomposition with applications in subspace-based algorithms," *IEEE Transactions on Signal Processing*, vol. 50, no. 11, pp. 2820–2830, 2002.
- [28] D. R. Brillinger, *Time Series: Data Analysis and Theory*, vol. 36 of *Classics in Applied Mathematics*, SIAM, Philadelphia, Pa, USA, 2001.

Foundation, Germany, the 2002 Young Explorers Prize from the Canadian Institute for Advanced Research (CIAR), and the 2000 Premier's Research Excellence Award, Ontario, Canada. He is currently Editor-in-Chief of the *IEEE Signal Processing Letters*. He was Associate Editor of the *IEEE Transactions on Signal Processing* (1999–2006). He is on Editorial Boards of *EURASIP Journal on Wireless Communications and Networking* and *EURASIP Signal Processing Journal*. He is Vice-Chair of the Sensor Array and Multichannel (SAM) Technical Committee (TC) of the IEEE Signal Processing Society.

Keyvan Zarifi received his B.S. and M.S. degrees both in electrical engineering from University of Tehran, Tehran, Iran, in 1997 and 2000, respectively. From January 2002 until March 2005, he was with the Department of Communication Systems, University of Duisburg-Essen, Duisburg, Germany. From April 2005, he has been with the Department of Communication Systems, Darmstadt University of Technology, Darmstadt, Germany, where he currently pursues his Ph.D. From September 2002 until March 2003, he was a Visiting Scholar at the Department of Electrical and Computer Engineering, McMaster University, Hamilton, Ontario, Canada. His research interests include statistical signal processing, multiuser detection, blind estimation techniques, and MIMO communications.



Alex B. Gershman received his Diploma and Ph.D. degrees in radiophysics and electronics from the Nizhny Novgorod State University, Russia, in 1984 and 1990, respectively. From 1984 to 1999, he held several full-time and visiting research appointments in Russia, Switzerland, and Germany. In 1999, he joined the Department of Electrical and Computer Engineering, McMaster University, Hamilton, Ontario, Canada, where he became a Full Professor in 2002. From April 2005, he has been with the Darmstadt University of Technology, Darmstadt, Germany, as a Professor and Head of the Communication Systems Group. His research interests span the areas of signal processing and communications with primary emphasis on statistical signal and array processing, adaptive beamforming, MIMO and space-time communications, multiuser and multicarrier communications, radar and sonar signal processing, and estimation and detection theory. He received the 2004 IEEE Signal Processing Society Best Paper Award. He is a Fellow of the IEEE and a recipient of the 2001 Wolfgang Paul Award from the Alexander von Humboldt

